Electronic and vibrational contributions to the reorganization energy of photosynthetic pigments

Cassiano, Tiago de Sousa Araújo; de Sousa, Leonardo Evaristo; Gargano, Ricardo; Neto, Pedro Henrique de Oliveira

Published in:
Chemical Physics Letters

Link to article, DOI:
10.1016/j.cplett.2023.140384

Publication date:
2023

Document Version
Publisher's PDF, also known as Version of record

Chemical Physics Letters 815 (2023) 140384

Contents lists available at ScienceDirect

Chemical Physics Letters

journal homepage: www.elsevier.com/locate/cplett

Research paper

Electronic and vibrational contributions to the reorganization energy of photosynthetic pigments

Tiago de Sousa Araújo Cassiano [a], Leonardo Evaristo de Sousa [b,*], Ricardo Gargano [a], Pedro Henrique de Oliveira Neto [a]

[a] Institute of Physics, University of Brasilia, 70919-970, Brasilia, Brazil
[b] Department of Energy Conversion and Storage, Technical University of Denmark, Denmark

GRAPHICAL ABSTRACT

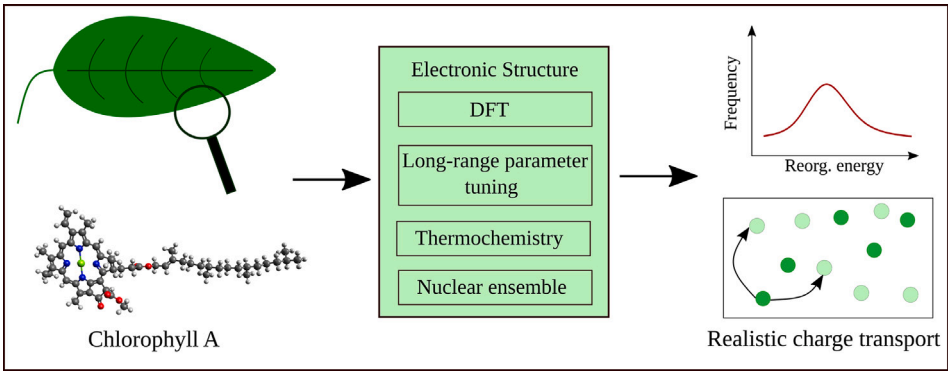

HIGHLIGHTS

- Hole and electron reorganization energies are calculated for a series of molecules of interest to photosynthesis.
- Improvements in the method of calculation of these energies are presented.
- Vibrational effects are accounted for using an ensemble method.
- These effects may have important consequences to charge transport in molecules.

ARTICLE INFO

Keywords:
DFT
Photosynthesis
Charge transfer
Reorganization energy

ABSTRACT

Charge transport is dependent on properties such as reorganization energy (λ) and free energy. These quantities are typically estimated applying density functional theory (DFT) to optimized geometries. However, most pigments in photosynthesis are conjugated, making delocalization and vibrational effects relevant. Here, we calculated reorganization energies of 15 molecules relevant to photosynthesis using a reliable DFT-based approach. Tuning the functional's long-range parameter prevents over-delocalization of orbitals, while molecular vibrations are accounted for via an ensemble method. Results show that functional tuning decreases λ, but vibrational effects produce distributions of λ, affecting charge transfer rates in up to one order of magnitude.

* Corresponding author.
E-mail address: ledso@dtu.dk (L.E. de Sousa).

https://doi.org/10.1016/j.cplett.2023.140384
Received 6 December 2022; Received in revised form 6 February 2023; Accepted 14 February 2023
Available online 16 February 2023

1. Introduction

Photosynthesis is the most important organic-driven energy conversion process on Earth [1,2]. The organisms that rely on it are the foundation of almost every biome. In that sense, there is a massive effort directed to unveil this complex reaction, conferring it a paramount role in the theoretical and applied fields as inspiration to the design of breakthrough applications [3–6]. It can also serve as object for studies regarding light absorption [7,8], charge dynamics [9,10] and protein dynamics [11–13]. In the case of applied works, most of the effort aims to mimic photosynthesis artificially using alternative compounds, potentially leading to a clean and unrestricted energy source [14–16]. In practice, photosynthesis consists of successive reactions mainly driven by highly specialized pigments that were finely selected through over 3.5 billion years of continuous sophistication and adaptation [17]. Understanding the properties of these compounds can not only provide a better description of photosynthesis but give new insights for future application designs as well. Towards this goal, a detailed and reliable investigation of photosynthetic pigments is imperative.

The reaction begins inside light-harvesting complexes [8,18] where pigments absorb energy from incident light and store it in the form of an excited electronic state known as exciton, a bosonic chargeless bound state of an electron and a hole. This quasiparticle drifts in the region through a process known as the resonance energy transfer mechanism [19]. The excitations that do not suffer recombination may reach a specialized chlorophyll inside the reaction center. There, some of the excitons suffer charge separation, generating free holes and electrons that now move via a charge-transfer process. The hopping continues until the charges reach key agents that will trigger a series of chemical reactions to store energy in the form of chemicals.

Throughout those steps, auxiliary pigments assist the reaction's course through specific functions [11,18]. In the light absorption step, the chromophores can act as antennas, absorbing light in complementary frequencies bands not covered by chlorophyll. Eventually, excitons created in these individuals follow the same path towards the reaction center, improving the light energy intake. Another role is photo-protection, in which the pigments prevent damage in the case of excessive light exposure or when there are triplet excitons in chlorophyll. In such cases, the chromophores can quench the potentially damaging excitation away from the primary pigments [20,21] and dissipate it through non-radiative decay, converting the energy into heat. Moreover, the agents outside the reaction center form a spatial-energetic funnel towards this region, effectively trapping the quasiparticles to prevent energy loss [22,23]. Interestingly, some molecules can even perform multiple tasks. For instance, lutein can aid the absorption of light or act as a photo-protector, depending on subtle changes in its conformation provided by surrounding proteins [24] inside the light-harvesting complex II, a membrane protein specialized on harvesting energy. All in all, these compounds are responsible for implementing photosynthesis. Because of that, a detailed examination of the electronic properties regarding their roles is crucial for understanding such complex mechanisms.

The charge dynamics mechanism is pivotal after the charge separation step. From the theoretical standpoint, Marcus' theory may be applied to describe the charge transfer processes between organic compounds. According to this model, the hopping rate depends on the reorganization energy (λ), a physical quantity that estimates the energy relaxation cost of transferring charge into molecules. This quantity can be estimated using density functional theory (DFT) through the calculation of the energies of frozen geometries in the neutral and charged states. However, it is well known that hybrid functionals in DFT enforce a non-physical trend of delocalizing molecular orbitals [25–27]. This effect is even more prominent in large and conjugated molecules [28], which is the very case of the pigments present in photosynthesis. In addition, vibrational effects are potentially relevant as well. Organic compounds, especially large and conjugated, are intrinsically malleable. In such cases, the assumption that electronic transitions do not significantly alter the nuclear conformation, known as the Franck–Condon principle, does not hold. Intra- and inter-molecular vibration contributions to the charge transport parameters were extensively studied in the past, revealing that the mechanism has a high sensitivity to them, depending on the type of crystal structure [29]. Theoretical reports have proposed numerous strategies to include these effects, namely extracting distributions of the electronic coupling from molecular mechanics [29], using the Marcus–Levich–Jortner rate equation [30,31] or calculating the local and nonlocal electron–phonon coupling terms [32–37]. For those reasons, the standard procedure of estimating λ may not be suitable for photosynthetic materials, requiring a more refined approach. Here we deliver an alternative protocol to estimate adequately the reorganization energy of highly conjugated molecules.

In this work, we calculated the electron and hole reorganization energies of 15 pigments commonly present in photosynthesis via DFT while accounting for vibrational and delocalization effects. First, we estimated λ via the conventional four-point geometry approach, serving as a reference. Next, the orbital's delocalization error is treated by tuning the functional's long-range parameter (ω) so that the Koopmans theorem stands valid for each compound, allowing us to reevaluate λ. Nowadays, its use is widely spread in quantum chemistry, being present in diverse DFT-based investigations for precision gains [38–41]. Results show that λ drops systematically about 22% in all pigments after enforcing the ω tuning, showing a significant difference from standard techniques. Moreover, the agreement with experimental results [42] validates this methodology and reveals the importance of carrying out the tuning procedure. We considered the vibrational character of the molecules by employing the nuclear ensemble method, which uses the molecule's modes of vibration to construct the geometry ensembles, giving rise to distributions of λ. Our analysis shows that the molecule's vibration can lead to substantial variability for the λ, suggesting that the calculations that return only averaged values of λ are potentially oversimplifying the physical description of charge transfer in photosynthetic pigments. Finally, the Gibbs free energy difference upon charge transfer is also provided, indicating the reaction's preferable path. Interestingly, we found that chlorophylls tend to favor the transfer of specific types of charge carriers. In addition, the hopping of hole and electron transfer reactions with the same reagents follow a tendency to fall into different reaction paths, promoting higher degrees of charge separation, which ultimately contributes to reducing energy loss over exciton recombination. We believe that is a consequence of the sophisticated selection of pigments throughout the evolutionary development of photosynthesis.

2. Methodology

2.1. Charge hopping rate

The charge transfer reaction between an acceptor molecule (**A**) and a donor (**D**) without auxiliary agents is

$$\mathbf{A} + \mathbf{D}^{+/-} \rightarrow \mathbf{A}^{+/-} + \mathbf{D}, \tag{1}$$

where $+/-$ represents the species hosting hole/electron carriers [43]. According to Marcus Theory [44,45,45–47], the charge hopping rate under the fixed site regime [48] is given by

$$k = A \exp\left(-\frac{(\lambda + \Delta G)^2}{4\lambda k_B T}\right). \tag{2}$$

A is a term that depends on the molecules' electronic coupling, T corresponds to the system's temperature, k_B is the Boltzmann constant and ΔG is the Gibbs free energy of activation between the products and reactants. Finally, λ denotes the reorganization energy [45].

Fig. 1(a) illustrates the procedure to calculate λ according to the four-point method by representing the four geometries of interest in the potential energy surfaces (PES) of a hypothetical molecule "A".

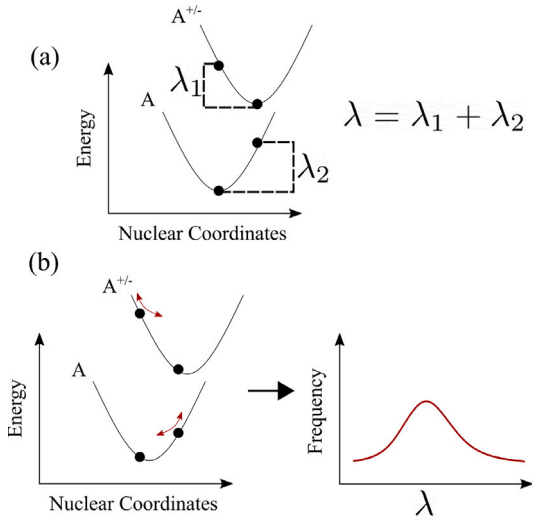

Fig. 1. Illustration of the approaches used in this work to estimate self-exchange λ for a given molecule **A**: (a) the conventional four-point method, (b) our proposed approach based on the nuclear ensemble formalism. In both figures, the neutral and charged PES are represented by parabolic-like curves indexed respectively by **A** and $\mathbf{A}^{+/-}$. The method in (a) requires the energy in four states, which are summed out to give an estimate of λ neglecting any vibrational effect. On the other hand, the procedure in (b) considers non-adiabatic configurations of the states E_N^C and E_C^N, represented by the red arrows in the SEPs, returning a distribution of λ.

The upper and lower parabolas depict the PES of neutral and charged configurations, respectively. Each curve has two points that represent the molecule's geometries of interest. The points at the center of the parabolas are the optimized conformations, namely E_N^N for the neutral curve and E_C^C for the charged one. Vertically aligned to them, are E_N^C and E_C^N. The former is the energy of the charged molecule at the neutral geometry, while the latter is the same for the neutral molecule at the charged geometry. Both states have the same geometries as their optimized counterparts, indicating an adiabatic charge change keeping the nuclear coordinates frozen. Then, the self-exchange λ is estimated as [43,46,49,50]:

$$\lambda = (E_C^N - E_N^N) + (E_N^C - E_C^C). \tag{3}$$

Moreover, it is customary to define λ over the sum of two intermediate relaxations $\lambda_1 = E_N^C - E_C^C$ and $\lambda_2 = E_C^N - E_N^N$. Naturally, the concept of reorganization energy is valid for both types of charge carriers. With that in mind, from now on, the λ of electron and hole will be denoted as λ_e and λ_h, respectively.

2.2. Nuclear ensemble

The vibrational motion of a molecule with N_a atoms is modeled as a system of $3N_a - 6$ uncoupled quantum harmonic oscillators. According to the quantum statistical mechanics, the normalized probability density of finding the ith normal mode quantum harmonic oscillator, at temperature T, dislocated from its equilibrium by R_i is:

$$\rho_i = \left(\frac{\mu_i \eta_i}{2\pi\hbar \sinh(\hbar\eta_i/k_bT)}\right)^{1/2} \times \\ \times \exp\left(-\frac{\eta_i\mu_i}{\hbar} R_i^2 \tanh\left(\frac{\hbar\eta_i}{2k_bT}\right)\right), \tag{4}$$

where μ_i and η_i are respectively the reduced mass and angular frequency of the ith mode, k_b is the Boltzmann constant and $\hbar$ is the reduced Planck constant.

Consequently, the probability density of having the molecule shifted by an arbitrary displacement becomes:

$$\rho(\vec{R}, T) = \prod_{i=1}^{3N_a-6} \rho_i. \tag{5}$$

Here, $\vec{R}$ is the displacement vector that shifts the molecule from its equilibrium, being the result of dislocating the atoms by all R_i's along their corresponding normal mode coordinates.

With Eq. (5) it is possible to obtain an ensemble of geometries of a given molecule at some defined temperature. This is done by sampling R_is from the Gaussian distributions of Eq. (4) for each ith normal mode [51]. Then, one transforms these displacements to the real space, translating into the conformal changes for the molecule. The process is repeated until the desired number of geometries is produced, giving rise to an ensemble of geometries. Finally, averaging some physical quantity over the ensemble permits the estimation of the vibrational contribution.

In our case, we will employ the nuclear ensemble formalism to extend Eq. (3). The four-point method assumes that the relaxation due to charge transfer occurs in an adiabatic manner, where the geometries of the states E_N^C and E_C^N are the same as the conformations at equilibrium. We will remove this restriction by allowing the states' geometries to oscillate around the optimized configuration, as shown in Fig. 1(b). The points corresponding to the states E_N^C and E_C^N have red arrows around them, illustrating the access of other geometries near-equilibrium via the nuclear ensemble. Let N be the number of conformations composing each ensemble of these states. Then, the procedure will generate N independent values of λ_1 and λ_2. According to Eq. (3), λ is the sum of these two quantities. Therefore, all possible combinations between the N λ_1s and the N λ_2s should be accounted for on equal footing, resulting in a distribution of λ with N^2 occurrences. On the right side of Fig. 1(b), the procedure is shown, as it illustrates the distribution of λ resulting from the contribution of the normal modes. For the ensemble extension of Eq. (3), we used the corresponding most stable ensemble-generated conformations as the optimized geometries E_N^N and E_C^C.

Finally, we stress that there is a great diversity of photosynthetic organisms. Consequently, photosynthesis is conceivable through multiple pigment profiles. However, it is beyond the scope of this work to investigate the inner mechanisms of each individual pigment profile. Instead, we provide a broader approach that considers some of the most relevant pigments without restricting the analysis to specific cases to deliver more general insights into photosynthesis.

3. Computational details

Calculations were run for 15 molecules, whose molecular structures are displayed in the supporting information file. Figures S1 (a), (b), (c) and (d) show chlorophyll A, chlorophyll B, chlorophyll C1 and pheophytin A structures, respectively. Similarly, antheraxanthin (a), canthaxanthin (b), neoxanthin (c), lutein (d), violaxanthin (e) and zeaxanthin (f) are displayed in Figure S2. Finally, Figure S3 illustrates 3-Hydroxyechinenone (a), Dihydrobiliverdin (b), Peridinin (c), Phycocyanobilin (d) and β-carotene (e) compounds.

All electronic structure calculations were performed using the Gaussian 16 software [52] with the ωb97xd/6-31G(d,p) [53] level of theory. Normal mode analysis was performed after all optimizations to ensure that the optimized structures corresponded to minima of the PES. The ω tuning and nuclear ensemble procedures were implemented using LeoX software [54,55]. The ensembles are generated at 300 K. Importantly, single-point calculations on ensemble geometries made use of the polarizable continuum model (PCM), as it is a standard approach to account for the medium's effect on the molecule's electronic structure [56–59]. As we focus on intramolecular properties, we refrain from analyzing outer-sphere contributions to reorganization energies in this work. The chosen solvent has a dielectric constant of 3.24, representing the interior of proteins on a typical biological environment [60–62]. However, we highlight that the dielectric constant can significantly change, depending on the local surroundings in photosynthesis [63]. The implications of this effect fall outside the main goal of this work. Here, the parameter will be restricted to a single value to give an approximate response. Finally, details of the ω tuning procedure and the estimate of ΔG can be found in the supporting information file.

Table 1
Hole and electron reorganization energies ($\lambda_{h/e}$) without and with the tuning of the long-range parameter. Molecules that belong to the chlorophyll group are highlighted in light green, while the xanthophyll compounds are in light blue.

	λ_e (eV)		λ_h (eV)	
Molecules	Non-tuned	Tuned	Non-tuned	Tuned
Chlorophyll A	0.40	0.32	0.25	0.22
Chlorophyll B	0.37	0.30	0.34	0.30
Chlorophyll C1	0.34	0.30	0.33	0.28
Pheophytin A	0.47	0.36		
Antheraxanthin	0.70	0.53	0.70	0.53
Canthaxanthin	0.87	0.69	0.65	0.44
Neoxanthin	1.02	0.81	0.83	0.65
Lutein	0.70	0.52	0.68	0.50
Violaxanthin	0.80	0.54	0.76	0.49
Zeaxanthin	0.77	0.60	0.73	0.57
3-Hydroxye.	0.85	0.64	0.69	0.49
Dihydrobiliverdin	0.57	0.48	0.88	0.76
Peridinin	0.77	0.62	0.65	0.51
Phycocyanobilin	1.10	0.90	1.14	0.88
β-carotene	0.69	0.52	0.73	0.56

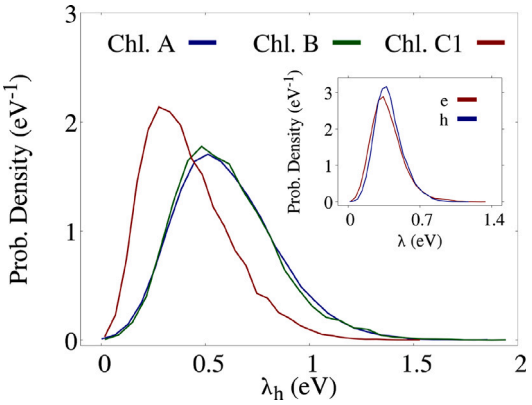

Fig. 2. Distribution of λ_h for Chlorophyll A (blue), B (green) and C1 (red). The inset displays distributions of both λ_h and λ_e for antheraxanthin.

4. Results

Table 1 displays the self-exchange hole and electron reorganization energies calculated via the four geometry points given by Eq. (3) with the ωb97xD's original range-separation parameter and its non-empirically tuned counterpart. In all cases the λ values range between 0.2 to about 1 eV. However, the tuning procedure results in a consistent drop of about 22% when compared with the standard method. Importantly, analysis of experimental results shows that the difference represents a direct precision gain for the calculations. For instance, β-carotene λ_h is experimentally estimated as 0.4 ∓ 0.03 eV [42]. Our calculation yielded 0.56 eV, while the standard functional returns 0.69 eV. Likewise, zeaxanthin's λ_h is experimentally estimated at 0.39 ∓ 0.04 eV and our calculations yielded 0.57 eV. Both cases show expressive reductions of λ towards the experimental result. Therefore we conclude that the non-physical delocalization of electron density can result in overestimation of λ, which can be corrected by the ω-tuning procedure, as described in the supporting information file.

Table SI shows the tuned values of the long-range parameter. While most of the tuned parameters are near 0.12 $(a_0)^{-1}$, the ωB97XD's ω default value is 0.2 $(a_0)^{-1}$ [53]. This systematic decrease of ω is effectively extending the short-range region in the computation of Coulomb potential [64]. As a result, close examination of the energies obtained with tuned functionals shows that all E_N^N, E_N^C, E_C^C, and E_C^N energies decreased when compared to those obtained with the default ω value. However, the changes in energies obtained for the out-of-equilibrium calculations (E_N^C and E_C^N) are greater in magnitude than those observed in the equilibrium calculations (E_N^N and E_C^C), resulting in lower reorganization energies.

The calculated λs using PCM and the relative ratios between the tuned ω and the functional's default value are also presented in Table SI. It is worth noting that comparison with the tuned results of Table 1 reveals that PCM does not alter significantly the λ estimate.

Interestingly, a theoretical report using B3LYP/6-31G** level theory reached β-carotene, chlorophylls A, B, and C1 λ values significantly closer to the ones obtained here through the ω-tuning [65]. To give an example, they found the hole and electron chlorophyll A λ equal to 0.2 eV and 0.33 eV, respectively. Although the estimates via B3LYP agree well with our results, we recall that this functional carries a well-known nonphysical tendency to over-delocalize the wave functions, which underestimates the torsion potentials, bond-length alternations and overestimates conjugation [66,67]. Besides, the energy of charge-transfer states are strongly underestimated [66]. These limitations altogether severely affect the physical description of π conjugated molecules. On the other hand, the tuned long-range corrected functionals mitigate this problem, providing a better equilibrium between DFT and Hartree–Fock exchange contributions. We attribute the accordance reached by B3LYP calculations as the result of error cancellation.

Moreover, regardless of the carrier type, molecules of the chlorophyll type show a characteristic behavior that disconnects from the other pigments, having a significantly lower λ of about 0.35 eV. Such a result may be expected due to the roles played by these compounds at the reaction center [68]. During the energy conversion step, chlorophylls can act as a host for charge separation and as a target to charge transfer mechanisms. Therefore, one may expect lower λ values.

Alternatively, all the xanthophylls display higher readings for both carrier types, showing λs around 0.6 eV, suggesting that auxiliary pigments may have an additional role by offering a potential barrier that restricts charge hopping on them. The finding relates to the well-known functions of such compounds in photo-protection and energy dissipation [69]. To effectively perform these tasks, the pigments surround the reaction center, where charges must remain for optimized efficiency. Because their λ are significantly higher, this spatial configuration traps the carriers, limiting their leakage to regions outside the reaction center. This suggests that these pigments may have an additional role in photosynthesis as charge barricades. The trend of high λ holds for both hole and electron carriers, although λ may vary significantly, implying that the carrier type can influence the photosynthesis efficiency. An equivalent analysis extends to the other non-chlorophyll pigments. We emphasize that changes in electronic coupling due to vibrational effects are expected to be significant, as demonstrated in past works [29–31,34]. However, extending the work for the electronic coupling would require a separate investigation to model the fluctuations in intermolecular properties, such as relative orientation and acceptor–donor distances. Thus we focus not on evaluating charge transfer rates, but rather on assessing the effects of accounting for intramolecular vibrations which still provide insight into the overall charge transport mechanism.

We now move to the second improvement on calculating λ: the molecule's vibrational modes. The extension, given by the nuclear ensemble approach, ultimately returns a distribution of λ obtained by considering all possible settings between the picked geometries. Fig. 2 displays the distribution of λ_h for chlorophyll A (red), B (green), C1 (red). In all cases, the distributions are skewed gaussian-like. Particularly, chlorophyll A and B's curves share other similarities, as they are centering nearly at the same value and have comparable dispersion, implying accordance in λ as well. We emphasize that the standard procedure is not able to grasp this parallel. Additionally, chlorophyll C1's distribution centers in slightly lower values and presents a more modest dispersion. All these distribution-related observations exemplify the potential impact of the molecule's vibrational modes in the evaluation of λ.

Table 2
Average and standard deviation for electron ($\langle\lambda_e\rangle$, σ_e) and hole ($\langle\lambda_h\rangle$, σ_h) reorganization energies calculated from ensembles. Molecules that belong to the chlorophyll group are highlighted in light green, while the xanthophyll compounds are in light blue.

Molecules	$\langle\lambda_e\rangle \pm \sigma_e$ (eV)	$\langle\lambda_h\rangle \pm \sigma_h$ (eV)
Chlorophyll A	0.63 ± 0.25	0.63 ± 0.24
Chlorophyll B	0.70 ± 0.3	0.63 ± 0.24
Chlorophyll C1	0.59 ± 0.28	0.44 ± 0.20
Pheophytin A	0.72 ± 0.31	— ± —
Antheraxanthin	0.41 ± 0.16	0.42 ± 0.13
Canthaxanthin	0.44 ± 0.16	0.46 ± 0.16
Neoxanthin	0.46 ± 0.17	0.53 ± 0.18
Lutein	0.43 ± 0.12	0.41 ± 0.16
Violaxanthin	0.41 ± 0.15	0.44 ± 0.14
Zeaxanthin	0.46 ± 0.17	0.60 ± 0.25
3-Hydroxye.	0.40 ± 0.15	0.41 ± 0.16
Dihydrobiliverdin	0.39 ± 0.13	0.44 ± 0.27
Peridinin	0.48 ± 0.22	0.40 ± 0.19
Phycocyanobilin	0.48 ± 0.20	0.49 ± 0.21
β-carotene	0.36 ± 0.13	0.38 ± 0.14

The inset in Fig. 2 shows antheraxanthin's λ_h distribution. Here, the distribution still retains the skewed gaussian-like shape. More importantly, the type of charge carrier seems to not induce significant changes in the distribution, as their dispersions and peak positions are nearly the same. The result agrees with the previous trend observed in Table 1, where no relevant distinction can be made between antheraxanthin's λ_h and λ_e. Fig. S4 displays the same distribution for the molecules from xanthopyll group. As it can be seen, all of them share the same response, indicating that the self-exchange hopping has a low sensibility to the charge type.

Table 2 gathers the numerical data of the λ distributions for a more systematical analysis. The first column gives the ensemble's average of electron reorganization energy $\langle\lambda_e\rangle$ its standard deviation σ_e. The adjacent column display the same for the hole carrier, that is the ensemble's average of hole reorganization energy $\langle\lambda_h\rangle$ the corresponding standard deviation σ_h. The chlorophyll molecules are highlighted at the table in light green and the xanthophyll ones are in light blue.

Comparison with previous results reveals the impact of vibrational effects in our estimates. Regarding the chlorophylls, the ensemble averages are considerably bigger, regardless of the carrier type, if compared with the results from the four-point method with tuned ω. For instance, Table 1 shows that $\lambda_h = 0.22$ eV for chlorophyll A, while $\langle\lambda_h\rangle$ is found to be 0.63 eV with $\sigma_h = 0.24$ eV. The trend remains for the other chlorophyll molecules, where the means are about 50% greater than the four-point's results. On the other hand, the xanthophylls averages are considerably smaller than the previous estimate, amounting to a drop of about 10% for the hole and 28% for the electron. Canthaxanthin's and zeaxanthin's $\langle\lambda_h\rangle$ are the only cases in which the average is bigger than the four-point calculation, with both having a variation of approximately 5%. Therefore, accounting for the vibrational effects in these compounds can greatly affect their response to charge transport. Moreover, the results suggest that chlorophyll molecules are more sensitive to vibrational effects.

In addition, the corresponding standard deviation inserts variability to λ estimates. For all cases, σ is comparable with its respective mean, meaning that molecular flexibility can highly alter λ estimates. In that sense, methodologies based on only stationary conformations, might be oversimplifying the underlying charge hopping mechanism. One may note that σ is greater in chlorophyll molecules than in xanthophylls. This strengthens the previous observation that chlorophylls are more sensitive to changes due to vibration.

Due to the complexity of photosynthesis, it is still not clear how these wide variations may affect the overall mechanism. However, as a rough estimate, we calculate ratio between the ensemble-generated charge transfer k_{ens} and the one given by the four-point approach

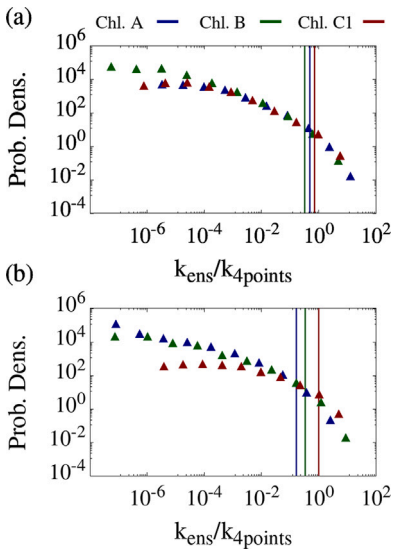

Fig. 3. Probability density distributions of the ratios between ensemble-generated (k_{ens}) hole (a) and electron (b) transfer rates and those calculated via the four-geometry method ($k_{4points}$). The blue, green and red points refer to Chlorophyll A, B and C1, respectively. The vertical lines indicate the mean ratio of the distributions with the corresponding colors.

$k_{4points}$ while neglecting vibrational contributions in the electronic coupling. Fig. 3 displays the distribution of $k_{ens}/k_{4points}$ for the chlorophyll compounds with electron (a) and hole (b) carriers. The plots have three vertical lines that indicate the ratio's mean of each corresponding compound.

As it can be seen, the distributions follow the same pattern. For small ratios, the probability density is high. Then, when the ratio increases, probability density decreases monotonically. We recall that, analogous to normal distributions, a more intense decline means a measure with greater variability. The molecules have similar behavior for both carriers, exhibiting a decay at nearly the same pace. Therefore, we conclude that vibrational effects provoke similar variability to the charge transfer rate for all chlorophylls. This is expected since the standard deviation is nearly the same among these compounds. Interestingly, the mean ratio is always smaller than 1 for all cases, meaning that vibrational effects tend to lower the rate compared with methods that use only stationary configurations. The intensity of this effect varies for each case. It can be small, as in the case of chlorophyll C1 hole that shows a ratio of 0.96. On the other hand, it can be as significant as seen in the case of chlorophyll A's hole which has a ratio of 0.16. Nevertheless, this puts a considerable variability in the charge transfer rate estimates of over one order of magnitude, which can dramatically affect the physical description in photosynthetic systems.

We can extend our analysis for xanthophyll molecules as well. Fig. 4 shows the distribution of the transfer rate ratios for violaxanthin (a), zeaxanthin (b), canthaxanthin (c), neoxanthin (d), antheraxanthin (e), and lutein (f). The distributions display the same shape found in the chlorophyll case. However, they decay at a faster pace now, suggesting that the charge transfer rate of these molecules suffers less variability than in chlorophylls. Interestingly, all of them have a mean ratio greater than 1, meaning that neglecting vibrational effects can underestimate the charge transfer rate in xanthophylls.

So far, the self-exchange λ was the basis for our analysis. Because of that, some of the insight regarding the interplay of the molecules was inevitably hidden. In this sense, the Gibbs free energy variation provides a simplified yet intuitive picture of the overall mechanism. For this reason, we calculated ΔG considering all possible combinations of acceptor/donor between the chosen molecules, following the methodology described in the supporting information text. Fig. 5 displays

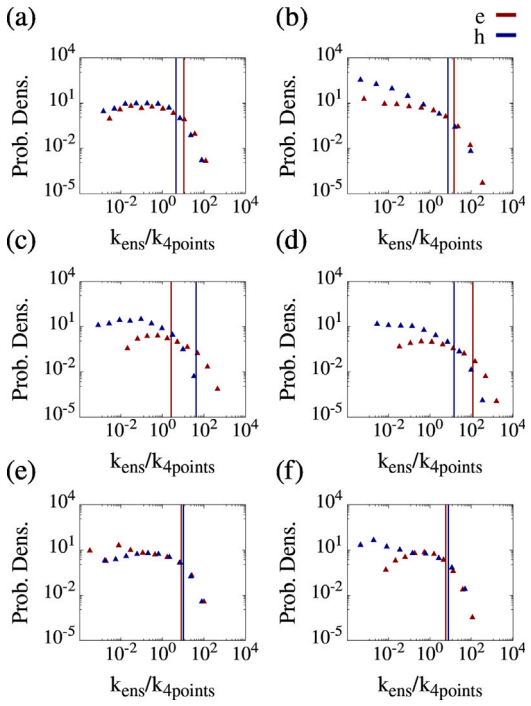

Fig. 4. Distribution of the ratio between the charge transfer rate given by the ensemble and the one calculated through the standard four-points method ($k_{ens}/k_{4points}$) for the violaxanthin (a), zeaxanthin (b), canthaxanthin (c), neoxanthin (d), antheraxanthin (e), and lutein (f). The red distribution refers to the electron case, while the blue one is from the hole.

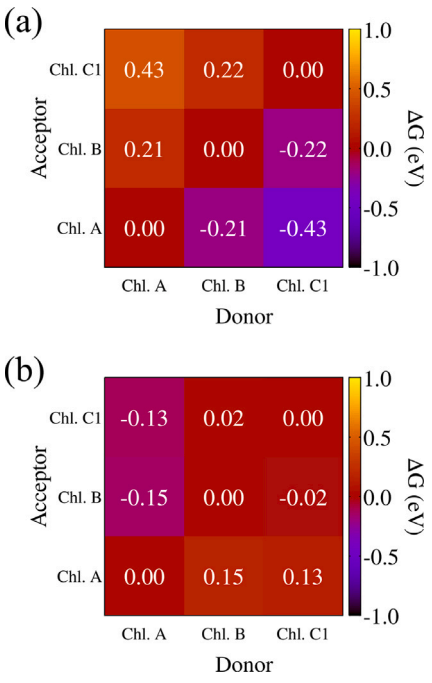

Fig. 5. Charge transfer's ΔG heatmaps between Chlorophyll molecules. The donor and acceptor compounds are placed in the horizontal and vertical axes, respectively. Light colors represent a positive free Gibbs variation for a given pair of reagents, indicating that the given reaction path may not be spontaneous. Inversely, dark colors denote negative ΔG variations, suggesting a favorable path. (a) displays the heatmap for the hole carrier, while (b) corresponds to the electron.

heatmaps of ΔG between chlorophyll specimens for the hole (a) and electron (b) carriers. The colors represent both the magnitude and sign of Gibbs's free energy. Dark tones refer to $\Delta G < 0$ while the light ones denote the opposite. Both heatmaps are symmetric along the diagonal as ΔG will change only its sign as the acceptor/donor roles are exchanged.

Interestingly, each chlorophyll displays an individual response depending on which compound they pair with and the carrier type. For the hole, ΔG is positive when chlorophyll C1 acts as an acceptor. This implies that the compound will likely not receive a hole carrier from other chlorophylls unless an additional source of energy balances the reaction enforcing this path. Alternatively, due to the symmetry mentioned, hole transfer from chlorophyll C1 to the other pigments may occur spontaneously. Inversely, chlorophyll A seems to respond oppositely, favoring the acceptance of hole, while chlorophyll B interacts differently depending on the pairing molecule. However, as we look at the electron carrier case, some observations are turned upside down. The reaction's ΔG with chlorophyll C1 as an acceptor and chlorophyll A as a donor is negative. A similar change occurs with charge transfer between chlorophylls A and B. In light of these observations, we conclude that charge transfer between the chlorophylls tends to physically separate the electron–hole pair since the reaction transfer of a charge carrier with negative ΔG is associated with a spontaneous transfer through the opposite path by the other carrier. An electron–hole pair scattering has a clear efficiency result: physically separating the two charges minimizes the chance of recombination. If recombination is reduced, less energy will be lost in the form of recombined excitons that would eventually decay through non-radiative or fluorescence processes. Therefore, the charge transfer reaction's ΔG between these compounds can be an evolutionary design aiming at photosynthesis optimization.

Figs. S5 and S6 display the heatmaps of ΔG for the hole and electron carriers, respectively. The colors have the same meaning as the last figure. The graphs show the overall picture regarding the path reaction of the studied compounds. In the hole case, ΔG is always positive when chlorophylls act as the acceptors for the other pigments. The behavior inverts if the carrier becomes the electron. Now, almost all pairing with accepting chlorophylls returns a negative ΔG. This suggests that, under such configurations, chlorophylls are more likely to take away the electrons from the other pigments, while surrendering the hole to them. Ultimately, the two effects combined should enhance charge efficiency by limiting the recombination process in the same fashion observed among the chlorophylls.

5. Conclusion

In summary, we calculated the hole/electron self-exchange reorganization energies of 15 pigments present in the photosynthesis while correcting the DFT's wave function over-delocalization problem via the ω-tuning. Comparison with standard methodologies reveals a significant drop in λ of about 22% for most of the compounds, showing that the physical description of the charge transfer mechanism can be severely affected if one does not balance properly the DFT and Hartree–Fock exchange contributions. Moreover, we observed that PCM does not affect significantly the estimations. Further analysis also shows that primary pigments have significantly lower λs when compared with the other compounds. Because the auxiliary molecules physically surround the light-harvesting complex, this suggests the existence of an energetic barrier that prevents the charge to emigrate away from the region. We believe that is an evolution-driven design to ensure energy conversion efficiency.

Next, we implemented an alternative way to calculate λ considering the molecule's vibrational modes, giving rise to a distribution of possible values. Unexpectedly, the ensembles' means significantly differ from the tuned four-point geometry approach results. Moreover, all cases present a significant deviant error, revealing an intrinsic and relevant variability to λ for those pigments. Consequently, some qualitative observations were only possible through the analysis of these

distributions. That suggests that theoretical and experimental methodologies based on single-valued reorganization energy are potentially over-simplifying the charge transfer mechanism. For a more tangible gauge of the impact of vibrational effect, it is desirable to unravel charge dynamics simulations that can implement the distribution of λ. Nevertheless, rough estimations show that the variability in the reorganization energy may represent changes of about one order of magnitude to the charge transfer rate. Interestingly, chlorophyll molecules display greater vibrational sensibility than xanthophylls. Therefore accounting for such effects can improve the physical description of charge transfer, providing a more reliable model for charge transport in photosynthesis.

Finally, we also estimated the Gibbs free energy variation over charge transfer between the pigments. Analysis of the pairing between the chlorophylls reveals that the spontaneous reaction path tends to be reversed when the carrier is switched from electron to hole or vice-versa. Ultimately, this can lead to spontaneous charge separation between electrons and holes, limiting the possibility of recombination and promoting efficiency. Such results indicate another evolutionary-driven design trend that selects compounds with the path reaction inversion property. Overall, the work represents an improved methodology to calculate reorganization energy for long and highly conjugated molecules. In addition, the design trends identified may inspire future developments in the research of artificial photosynthesis.

CRediT authorship contribution statement

Tiago de Sousa Araújo Cassiano: Conceptualization, Methodology, Software, Formal analysis, Validation, Writing – original draft. **Leonardo Evaristo de Sousa:** Conceptualization, Methodology, Formal analysis, Writing – review & editing, Visualization, Supervision. **Ricardo Gargano:** Methodology, Formal analysis, Writing – review & editing, Funding acquisition. **Pedro Henrique de Oliveira Neto:** Methodology, Conceptualization, Formal analysis, Resources, Writing – review & editing, Visualization, Supervision, Funding acquisition.

Declaration of competing interest

The authors declare that they have no known competing financial interests or personal relationships that could have appeared to influence the work reported in this paper.

Data availability

Data will be made available on request.

Acknowledgments

The authors thank Amanda Queiroz Sena for the productive discussions and helpful insights. This work was supported by the financial support from Brazilian Research Councils CNPq, (grant. number 304637/2018–1) CAPES, Brazil, and FAPDF, Brazil. P.H.O.N acknowledge the financial support from FAPDF, Brazil grants 00193.00001217/2021-13. L.E.S. acknowledges support by a research grant (00028053) from VILLUM FONDEN, Denmark.

Supporting information

Optimized geometries and details regarding ΔG and ω-tuning are available as supporting information.

Appendix A. Supplementary data

Supplementary material related to this article can be found online at https://doi.org/10.1016/j.cplett.2023.140384.

References

[1] Petra Fromme, Ingo Grotjohann, Overview of photosynthesis, in: Photosynthetic Protein Complexes: A Structural Approach, Wiley Online Library, 2008, pp. 1–22.
[2] Chenglong Wang, Da Xing, Qun Chen, A novel method for measuring photosynthesis using delayed fluorescence of chloroplast, Biosens. Bioelectron. 20 (3) (2004) 454–459.
[3] Oluwaseun Adedokun, Olufunke Lydia Adedeji, Ismaila Taiwo Bello, Mojoyinola Kofoworola Awodele, Ayodeji Oladiran Awodugba, Fruit peels pigment extracts as a photosensitizer in ZnO-based dye-sensitized solar cells, Chem. Phys. Impact 3 (2021) 100039.
[4] David O. Hall, Sergei A. Markov, Yoshitomo Watanabe, K. Krishna Rao, The potential applications of cyanobacterial photosynthesis for clean technologies, Photosynth. Res. 46 (1) (1995) 159–167.
[5] Teera Butburee, Pongkarn Chakthranont, Chaiyasit Phawa, Kajornsak Faungnawakij, Beyond artificial photosynthesis: prospects on photobiorefinery, ChemCatChem 12 (7) (2020) 1873–1890.
[6] Wenguang Tu, Yong Zhou, Zhigang Zou, Photocatalytic conversion of CO2 into renewable hydrocarbon fuels: state-of-the-art accomplishment, challenges, and prospects, Adv. Mater. 26 (27) (2014) 4607–4626.
[7] Qingyuan Zhang, Xiangming Xiao, Bobby Braswell, Ernst Linder, Fred Baret, Berrien Moore III, Estimating light absorption by chlorophyll, leaf and canopy in a deciduous broadleaf forest using MODIS data and a radiative transfer model, Remote Sens. Environ. 99 (3) (2005) 357–371.
[8] Souloke Sen, Vincenzo Mascoli, Nicoletta Liguori, Roberta Croce, Lucas Visscher, Understanding the relation between structural and spectral properties of light-harvesting complex II, J. Phys. Chem. A 125 (20) (2021) 4313–4322.
[9] S. Creighton, J.K. Hwang, A. Warshel, W.W. Parson, J. Norris, Simulating the dynamics of the primary charge separation process in bacterial photosynthesis, Biochemistry 27 (2) (1988) 774–781.
[10] Sujith Puthiyaveetil, Bart Van Oort, Helmut Kirchhoff, Surface charge dynamics in photosynthetic membranes and the structural consequences, Nat. Plants 3 (4) (2017) 1–9.
[11] Nicoletta Liguori, Roberta Croce, Siewert J. Marrink, Sebastian Thallmair, Molecular dynamics simulations in photosynthesis, Photosynth. Res. 144 (2) (2020) 273–295.
[12] Nicoletta Liguori, Pengqi Xu, Ivo H.M. Van Stokkum, Bart Van Oort, Yinghong Lu, Daniel Karcher, Ralph Bock, Roberta Croce, Different carotenoid conformations have distinct functions in light-harvesting regulation in plants, Nature Commun. 8 (1) (2017) 1–9.
[13] Sebastian Thallmair, Petteri A. Vainikka, Siewert J. Marrink, Lipid fingerprints and cofactor dynamics of light-harvesting complex II in different membranes, Biophys. J. 116 (8) (2019) 1446–1455.
[14] Biaobiao Zhang, Licheng Sun, Artificial photosynthesis: opportunities and challenges of molecular catalysts, Chem. Soc. Rev. 48 (7) (2019) 2216–2264.
[15] Ben Hankamer, Florian Lehr, Jens Rupprecht, Jan H. Mussgnug, Clemens Posten, Olaf Kruse, Photosynthetic biomass and H2 production by green algae: from bioengineering to bioreactor scale-up, Physiol. Plant. 131 (1) (2007) 10–21.
[16] Xu-Bing Li, Chen-Ho Tung, Li-Zhu Wu, Semiconducting quantum dots for artificial photosynthesis, Nat. Rev. Chem. 2 (8) (2018) 160–173.
[17] Robert E. Blankenship, Origin and early evolution of photosynthesis, Photosynth. Res. 33 (2) (1992) 91–111.
[18] Andreas Dreuw, Graham R. Fleming, Martin Head-Gordon, Chlorophyll fluorescence quenching by xanthophylls, Phys. Chem. Chem. Phys. 5 (15) (2003) 3247–3256.
[19] P.G. Wu, Ludwig Brand, Resonance energy transfer: methods and applications, Anal. Biochem. 218 (1) (1994) 1–13.
[20] Jonathan M. Morris, Graham R. Fleming, Quantitative modeling of energy dissipation in Arabidopsis thaliana, Environ. Exp. Bot. 154 (2018) 99–109.
[21] Peter Heathcote, Paul K. Fyfe, Michael R. Jones, Reaction centres: the structure and evolution of biological solar power, Trends Biochem. Sci. 27 (2) (2002) 79–87.
[22] Mykyta Onizhuk, Siddhartha Sohoni, Giulia Galli, Gregory S. Engel, Spatial patterns of light-harvesting antenna complex arrangements tune the transfer-to-trap efficiency of excitons in purple bacteria, J. Phys. Chem. Lett. 12 (29) (2021) 6967–6973.
[23] Robert E. Blankenship, Molecular Mechanisms of Photosynthesis, John Wiley & Sons, 2021.
[24] Minjung Son, Alberta Pinnola, Roberto Bassi, Gabriela S. Schlau-Cohen, The electronic structure of lutein 2 is optimized for light harvesting in plants, Chem 5 (3) (2019) 575–584.
[25] Tamar Stein, Leeor Kronik, Roi Baer, Reliable prediction of charge transfer excitations in molecular complexes using time-dependent density functional theory, J. Am. Chem. Soc. 131 (8) (2009) 2818–2820.
[26] Emil Proynov, Jing Kong, Correcting the charge delocalization error of density functional theory, J. Chem. Theory Comput. 17 (8) (2021) 4633–4638.
[27] Heather J. Kulik, Perspective: Treating electron over-delocalization with the DFT+ U method, J. Chem. Phys. 142 (24) (2015) 240901.
[28] Paula Mori-Sánchez, Aron J. Cohen, Weitao Yang, Localization and delocalization errors in density functional theory and implications for band-gap prediction, Phys. Rev. Lett. 100 (14) (2008) 146401.

[29] Nicolas G. Martinelli, Yoann Olivier, Stavros Athanasopoulos, Mari-Carmen Ruiz Delgado, Kathryn R. Pigg, Demétrio A. da Silva Filho, Roel S. Sánchez-Carrera, Elisabetta Venuti, Raffaele G. Della Valle, Jean-Luc Brédas, et al., Influence of intermolecular vibrations on the electronic coupling in organic semiconductors: the case of anthracene and perfluoropentacene, ChemPhysChem 10 (13) (2009) 2265–2273.

[30] Sofia Canola, Fabrizia Negri, Anisotropy of the n-type charge transport and thermal effects in crystals of a fluoro-alkylated naphthalene diimide: a computational investigation, Phys. Chem. Chem. Phys. 16 (39) (2014) 21550–21558.

[31] Simone Di Motta, Melania Siracusa, Fabrizia Negri, Structural and thermal effects on the charge transport of core-twisted chlorinated perylene bisimide semiconductors, J. Phys. Chem. C 115 (42) (2011) 20754–20764.

[32] Th Holstein, Studies of polaron motion: Part I. The molecular-crystal model, Ann. Physics 8 (3) (1959) 325–342.

[33] Roel S. Sánchez-Carrera, Pavel Paramonov, Graeme M. Day, Veaceslav Coropceanu, Jean-Luc Brédas, Interaction of charge carriers with lattice vibrations in oligoacene crystals from naphthalene to pentacene, J. Am. Chem. Soc. 132 (41) (2010) 14437–14446.

[34] Veaceslav Coropceanu, Roel S Sánchez-Carrera, Pavel Paramonov, Graeme M Day, Jean-Luc Brédas, Interaction of charge carriers with lattice vibrations in organic molecular semiconductors: naphthalene as a case study, J. Phys. Chem. C 113 (11) (2009) 4679–4686.

[35] Elham Mozafari, Sven Stafström, Polaron dynamics in a two-dimensional Holstein-Peierls system, J. Chem. Phys. 138 (18) (2013) 184104.

[36] Luiz Antonio Ribeiro Junior, Sven Stafström, Polaron stability in molecular semiconductors: theoretical insight into the impact of the temperature, electric field and the system dimensionality, Phys. Chem. Chem. Phys. 17 (14) (2015) 8973–8982.

[37] Jonathan H. Fetherolf, Denis Golež, Timothy C. Berkelbach, A unification of the Holstein polaron and dynamic disorder pictures of charge transport in organic crystals, Phys. Rev. X 10 (2) (2020) 021062.

[38] Seong bin Jo, Mina Ahn, Kamala Bhattarai, Kyung-Ryang Wee, Dae-Hwan Ahn, Jong-Won Song, UV/Vis absorption spectrum calculations of benzo-1,2-dipyrene isomer using long-range corrected density functional theory, Chem. Phys. Lett. 761 (2020) 138023.

[39] Corell Halsey-Moore, Puru Jena, James T. McLeskey Jr., Tuning range-separated DFT functionals for modeling the peak absorption of MEH-PPV polymer in various solvents, Comput. Theor. Chem. 1162 (2019) 112506.

[40] Kimihiko Hirao, Bun Chan, Jong-Won Song, Han-Seok Bae, Charge-transfer excitation energies expressed as orbital energies of Kohn–Sham density functional theory with long-range corrected functionals, J. Phys. Chem. A 124 (39) (2020) 8079–8087.

[41] Igo T. Lima, Andriele da S. Prado, Joao B.L. Martins, Pedro Henrique de Oliveira Neto, Artemis M. Ceschin, Wiliam F. da Cunha, Demetrio A. da Silva Filho, Improving the description of the optical properties of carotenoids by tuning the long-range corrected functionals, J. Phys. Chem. A 120 (27) (2016) 4944–4950.

[42] Hong Cheng, Rui-Min Han, Jian-Ping Zhang, Leif H. Skibsted, Electron transfer from plant phenolates to carotenoid radical cations. Antioxidant interaction entering the Marcus theory inverted region, J. Agricult. Food Chem. 62 (4) (2014) 942–949.

[43] Anup Thomas, Ramesh Kumar Chitumalla, Avinash L. Puyad, K.V. Mohan, Joonkyung Jang, Computational studies of hole/electron transport in positional isomers of linear oligo-thienoacenes: Evaluation of internal reorganization energies using density functional theory, Comput. Theor. Chem. 1089 (2016) 59–67.

[44] Rudolph A. Marcus, On the theory of electron-transfer reactions. VI. Unified treatment for homogeneous and electrode reactions, J. Chem. Phys. 43 (2) (1965) 679–701.

[45] Muhammet Erkan Köse, Kirk S. Schanze, Prediction of internal reorganization energy in photoinduced electron transfer processes of molecular dyads, J. Phys. Chem. A 124 (45) (2020) 9478–9486.

[46] Jean-Luc Brédas, David Beljonne, Veaceslav Coropceanu, Jérôme Cornil, Charge-transfer and energy-transfer processes in π-conjugated oligomers and polymers: a molecular picture, Chem. Rev. 104 (11) (2004) 4971–5004.

[47] David P. McMahon, Alessandro Troisi, Evaluation of the external reorganization energy of polyacenes, J. Phys. Chem. Lett. 1 (6) (2010) 941–946.

[48] Rudolph A. Marcus, Norman Sutin, Electron transfers in chemistry and biology, Biochim. Biophys. Acta (BBA) Rev. Bioenerg. 811 (3) (1985) 265–322.

[49] Sule Atahan-Evrenk, A quantitative structure–property study of reorganization energy for known p-type organic semiconductors, RSC Adv. 8 (70) (2018) 40330–40337.

[50] Ziran Chen, Yuan Li, Zhanrong He, Youhui Xu, Wenhao Yu, Theoretical investigations on charge transport properties of tetrabenzo [a, d, j, m] coronene derivatives using different density functional theory functionals (B3LYP, M06-2X, and wB97XD), J. Chem. Res. 43 (7–8) (2019) 293–303.

[51] Leonardo Evaristo de Sousa, Piotr de Silva, Unified framework for photophysical rate calculations in tadf molecules, J. Chem. Theory Comput. 17 (9) (2021) 5816–5824.

[52] M.J. Frisch, G.W. Trucks, H.B. Schlegel, G.E. Scuseria, M.A. Robb, J.R. Cheeseman, G. Scalmani, V. Barone, G.A. Petersson, H. Nakatsuji, X. Li, M. Caricato, A.V. Marenich, J. Bloino, B.G. Janesko, R. Gomperts, B. Mennucci, H.P. Hratchian, J.V. Ortiz, A.F. Izmaylov, J.L. Sonnenberg, D. Williams-Young, F. Ding, F. Lipparini, F. Egidi, J. Goings, B. Peng, A. Petrone, T. Henderson, D. Ranasinghe, V.G. Zakrzewski, J. Gao, N. Rega, G. Zheng, W. Liang, M. Hada, M. Ehara, K. Toyota, R. Fukuda, J. Hasegawa, M. Ishida, T. Nakajima, Y. Honda, O. Kitao, H. Nakai, T. Vreven, K. Throssell, J.A. Montgomery Jr., J.E. Peralta, F. Ogliaro, M.J. Bearpark, J.J. Heyd, E.N. Brothers, K.N. Kudin, V.N. Staroverov, T.A. Keith, R. Kobayashi, J. Normand, K. Raghavachari, A.P. Rendell, J.C. Burant, S.S. Iyengar, J. Tomasi, M. Cossi, J.M. Millam, M. Klene, C. Adamo, R. Cammi, J.W. Ochterski, R.L. Martin, K. Morokuma, O. Farkas, J.B. Foresman, D.J. Fox, Gaussian 16 Revision C.01, Gaussian Inc. Wallingford CT, 2016.

[53] Jeng-Da Chai, Martin Head-Gordon, Long-range corrected hybrid density functionals with damped atom–atom dispersion corrections, Phys. Chem. Chem. Phys. 10 (44) (2008) 6615–6620.

[54] Leonardo Evaristo de Sousa, LeoX, 2019, https://github.com/LeonardoESousa/LeoX.

[55] Leonardo Evaristo de Sousa, Fernando Teixeira Bueno, Geraldo Magela e Silva, Demétrio Antônio da Silva Filho, Pedro Henrique de Oliveira Neto, Fast predictions of exciton diffusion length in organic materials, J. Mater. Chem. C 7 (14) (2019) 4066–4071.

[56] Veaceslav Coropceanu, Xian-Kai Chen, Tonghui Wang, Zilong Zheng, Jean-Luc Brédas, Charge-transfer electronic states in organic solar cells, Nat. Rev. Mater. 4 (11) (2019) 689–707.

[57] Alfonso Pedone, Role of solvent on charge transfer in 7-aminocoumarin dyes: new hints from TD-CAM-B3LYP and state specific PCM calculations, J. Chem. Theory Comput. 9 (9) (2013) 4087–4096.

[58] Zilong Zheng, Jean-Luc Bredas, Veaceslav Coropceanu, Description of the charge transfer states at the pentacene/C60 interface: Combining range-separated hybrid functionals with the polarizable continuum model, J. Phys. Chem. Lett. 7 (13) (2016) 2616–2621.

[59] Valérie Vaissier, Piers Barnes, James Kirkpatrick, Jenny Nelson, Influence of polar medium on the reorganization energy of charge transfer between dyes in a dye sensitized film, Phys. Chem. Chem. Phys. 15 (13) (2013) 4804–4814.

[60] Koji Hasegawa, Takumi Noguchi, Density functional theory calculations on the dielectric constant dependence of the oxidation potential of chlorophyll: implication for the high potential of P680 in photosystem II, Biochemistry 44 (24) (2005) 8865–8872.

[61] Sérgio Filipe Sousa, Pedro Alexandrino Fernandes, Maria João Ramos, Gas-phase geometry optimization of biological molecules as a reasonable alternative to a continuum environment description: fact, myth, or fiction? J. Phys. Chem. A 113 (52) (2009) 14231–14236.

[62] Lev I. Krishtalik, Role of the protein's low dielectric constant in the functioning of the photosynthetic reaction center, Photosynth. Res. 60 (2) (1999) 241–246.

[63] C.S. Chamorovsky, S.K. Chamorovsky, A. Yu Semenov, Dielectric and photoelectric properties of photosynthetic reaction centers, Biochemistry (Moscow) 70 (2) (2005) 257–263.

[64] Laxman Pandey, Curtis Doiron, John S. Sears, Jean-Luc Brédas, Lowest excited states and optical absorption spectra of donor–acceptor copolymers for organic photovoltaics: a new picture emerging from tuned long-range corrected density functionals, Phys. Chem. Chem. Phys. 14 (41) (2012) 14243–14248.

[65] Farzaneh Zanjanchi, Javad Beheshtian, Natural pigments in dye-sensitized solar cell (DSSC): a DFT-TDDFT study, J. Iran. Chem. Soc. 16 (4) (2019) 795–805.

[66] Thomas Körzdörfer, Jean-Luc Bredas, Organic electronic materials: recent advances in the DFT description of the ground and excited states using tuned range-separated hybrid functionals, Acc. Chem. Res. 47 (11) (2014) 3284–3291.

[67] Jean-Luc Brédas, Organic electronics: does a plot of the HOMO–LUMO wave functions provide useful information? Chem. Mater. 29 (2) (2017) 477–478.

[68] Tanai Cardona, Arezki Sedoud, Nicholas Cox, A. William Rutherford, Charge separation in photosystem II: a comparative and evolutionary overview, Bioenergetics 1817 (1) (2012) 26–43.

[69] Peter Jahns, Alfred R. Holzwarth, The role of the xanthophyll cycle and of lutein in photoprotection of photosystem II, Bioenergetics 1817 (1) (2012) 182–193.